EUROPEAN HEMATOLOGY ASSOCIATION
haematologica
Journal of the European Hematology Association

Deficiency of the ribosome biogenesis gene *Sbds* in hematopoietic stem and progenitor cells causes neutropenia in mice by attenuating lineage progression in myelocytes

by Noemi A. Zambetti, Eric M. J. Bindels, Paulina M. H. Van Strien, Marijke G. Valkhof, Maria N. Adisty, Remco M. Hoogenboezem, Mathijs A. Sanders, Johanna M. Rommens, Ivo P. Touw, and Marc H. G. P. Raaijmakers

Haematologica 2015 [Epub ahead of print]

Citation: Zambetti NA, Bindels EM, Van Strien PM, Valkhof MG, Adisty MN, Hoogenboezem RM, Sanders MA, Rommens JM, Touw IP, and Raaijmakers MH. Deficiency of the ribosome biogenesis gene Sbds in hematopoietic stem and progenitor cells causes neutropenia in mice by attenuating lineage progression in myelocytes. Haematologica. 2015; 100:xxx
doi:10.3324/haematol.2015.131573

Deficiency of the ribosome biogenesis gene *Sbds* in hematopoietic stem and progenitor cells causes neutropenia in mice by attenuating lineage progression in myelocytes

Noemi A. Zambetti,[1] Eric M. J. Bindels,[1] Paulina M. H. Van Strien,[1] Marijke G. Valkhof,[1,2] Maria N. Adisty,[1] Remco M. Hoogenboezem,[1] Mathijs A. Sanders,[1] Johanna M. Rommens,[3] Ivo P. Touw,[1] and Marc H. G. P. Raaijmakers[1]

[1]Department of Hematology, Erasmus Medical Center Cancer Institute, Rotterdam, The Netherlands

[2]Current address: Laboratory for Cell Therapy, Sanquin Research and Landsteiner Laboratory, Amsterdam, The Netherlands

[3]Program in Genetics & Genome Biology, Peter Gilgan Centre for Research and Learning, The Hospital for Sick Children, Department of Molecular Genetics, University of Toronto, Toronto, ON, Canada

Running heads: *Sbds* deficiency in HSPC causes neutropenia in mice

Corresponding author: Marc H.G.P. Raaijmakers; e-mail: m.h.g.raaijmakers@erasmusmc.nl

Acknowledgments

The authors would like to thank Dr Marieke van Lindern and Roberto Avellino for valuable scientific discussions; Dr Kirsten van Lom, Marije Havermans, Dr Elwin Rombouts, Peter van Geel for technical assistance; and members of the Erasmus MC animal core facility EDC for the help with animal care. This work was supported by grants from the Dutch Cancer Society (KWF Kankerbestrijding), Amsterdam, The Netherlands (grant EMCR 2010-4733).

Abstract

Shwachman-Diamond syndrome is a congenital bone marrow failure disorder characterized by debilitating neutropenia. The disease is associated with loss-of-function mutations in the *SBDS* gene, implicated in ribosome biogenesis, but the cellular and molecular events driving cell specific phenotypes in ribosomopathies remain poorly defined. Here, we established, to our knowledge, the first mammalian model of neutropenia in Shwachman-Diamond syndrome through targeted downregulation of *Sbds* in hematopoietic stem and progenitor cells expressing the myeloid transcription factor CCAAT/enhancer binding protein α (*Cebpa*). *Sbds* deficiency in the myeloid lineage specifically affected myelocytes and their downstream progeny while, unexpectedly, it was well tolerated by rapidly cycling hematopoietic progenitor cells. Molecular insights provided by massive parallel sequencing supported cellular observations of impaired cell cycle exit and formation of secondary granules associated with the defect of myeloid lineage progression in myelocytes. Mechanistically, *Sbds* deficiency activated the p53 tumor suppressor pathway and induced apoptosis in these cells. Collectively, the data reveal a previously unanticipated, selective dependency of myelocytes and downstream progeny, but not rapidly cycling progenitors, on this ubiquitous ribosome biogenesis protein, thus providing a cellular basis for the understanding of myeloid lineage biased defects in Shwachman-Diamond syndrome.

Introduction

Shwachman-Diamond syndrome (SDS; OMIM 260400) is a rare congenital multi-systemic disorder characterized by exocrine pancreatic insufficiency, skeletal defects and bone marrow failure.[1-3] The hematological hallmark of the disease is neutropenia, which affects 88% to 98% of patients[4, 5] and represents, together with leukemic evolution, the main cause of morbidity and mortality in SDS.[1, 6-8] Other, less common manifestations are anemia, thrombocytopenia and pancytopenia.[6, 7] The disease is caused by biallelic loss of function mutations in the Shwachman-Bodian-Diamond Syndrome gene (*SBDS*).[9] The two most common mutations, 258+2T→C and 183-184TA→CT, result in impaired splicing and a premature stop codon, respectively, and are associated with reduced protein levels of SBDS.[9, 10]

SBDS plays an essential role in ribosome biogenesis. In particular, the concerted activity of SBDS and elongation factor-like 1 (EFL1) mediates the removal of eukaryotic initiation factor 6 (eIF6) during the cytoplasmic maturation of the pre-60S subunit, allowing the formation of the 80S ribosome.[10-12] Consistent with this notion, impaired ribosome subunit joining has been demonstrated in SDS patients[12, 13] and reduced overall translation was detected in yeast models of SDS.[11] Defects in ribosome biogenesis define a group of pathologies collectively known as ribosomopathies. Causative mutations in genes linked to ribosome biogenesis have been identified in several congenital diseases including Diamond-Blackfan anemia (DBA), dyskeratosis congenita and cartilage-hair hypoplasia. While the hematopoietic system is affected in most of these conditions, leading to some degree of bone marrow failure, pronounced vulnerability of specific cell lineages discerns these disorders, with neutropenia being the specific hallmark of SDS. This reflects the central enigma in the understanding of human congenital ribosomopathies, i.e. how disruption of ribosome biogenesis, a process occurring in all tissues with a proposed generic role in protein synthesis, results in cell and tissue specific disease phenotypes.

It is thought that ribosomes, and hence the proteins related to their biogenesis, are critically important for fast cycling cells, thus leading to impaired function of hematopoietic progenitor cells, resulting in cytopenia, but this view provides no explanation for cell type specificity (neutropenia) in SDS.[14, 15]

Identification of the cell types specifically affected by dysfunction of ribosomal genes will thus be critical in deciphering the underlying molecular mechanisms driving disease pathology, ultimately enabling targeted therapies. However, progress in understanding the pathophysiology of SDS is limited by the lack of a robust mammalian model faithfully recapitulating neutropenia. Deficiency of *Sbds* leads to embryonic lethality in full knockout mice[10, 16] and transplantation of shRNA-transduced, *Sbds*-deficient murine hematopoietic cells in wild type recipient mice did not result in overt neutropenia, although it impaired myeloid progenitor generation.[17] Targeting *Sbds* in the hematopoietic system via poly(I:C) treatment of *Sbds*$^{fl/-}$*Tg:Mx1-cre* mice resulted in a severe hepatic phenotype, precluding a thorough investigation of the hematological consequences of *Sbds* deficiency in adult hematopoietic stem cells (HSCs).[10] Thus, *in vivo* targeting of *Sbds* in postnatal mammalian hematopoiesis remains a key challenge for the field.

The basic leucine zipper transcription factor CCAAT/Enhancer-Binding Protein α (C/EBPα) is expressed in a fraction of HSCs and throughout the myeloid lineage,[18-20] thus offering an alternative approach to target hematopoietic stem and progenitor cells and their downstream myeloid lineage progeny in adult mammals.

Here, we generated a novel mouse model of genetic *Sbds* deletion through targeted downregulation of the gene in *Cebpa*-expressing cells, resulting in profound neutropenia. We show that loss of *Sbds* is well tolerated by rapidly cycling myeloid progenitor cells and identify myelocytes and their downstream progeny as the cell types within the hematopoietic hierarchy critically affected by *Sbds* deficiency through induction of cellular stress and apoptosis, thus providing a cellular and molecular basis for neutropenia in SDS.

Methods

Additional information is provided in the Online Supplement.

Mice and Genotyping

Cebpa$^{cre/+}$ R26 EYFP mice and *Sbds*$^{f/+}$ mice have been previously described.[19, 21] B6.SJL-*Ptprc*^{a}*Pepc*^{b}/BoyCrl (B6.SJL) mice were purchased from Charles River. Mice and embryos were genotyped by PCR on DNA isolated from toes and forelimbs, respectively, using the primers listed in Online Supplementary Table S1 (Life Technologies). Animals were maintained in specific pathogen free conditions in the Experimental Animal Center of Erasmus MC (EDC) and sacrificed by cervical dislocation. All animal work was approved by the Animal Welfare/Ethics Committee of the EDC in accordance with legislation in the Netherlands.

Fetal Liver Cell Transplantation

Fetal livers were isolated from E14.5 embryos. Cell suspensions were centrifuged, resuspended in a minimal volume of ACK lysing buffer (Lonza) and incubated on ice for 4 min to eliminate red blood cells. After centrifugation, cells were resuspended in PBS+0.5% FCS. 7-10-week-old, lethally irradiated (8.5Gy) B6.SJL mice were transplanted with $3x10^5$ fetal liver cells by tail vein injection. Recipients received antibiotics in the drinking water for 2 weeks after transplantation.

RNA Sequencing and GSEA Analysis

cDNA was synthesized and amplified using SMARTer Ultra Low RNA kit (Clontech Laboratories) following the manufacturer's protocol. Amplified cDNA was further processed according to TruSeq Sample Preparation v2 Guide (Illumina) and paired end-sequenced (2x75 bp) on the HiSeq 2500 (Illumina). Demultiplexing was performed using CASAVA software (Illumina) and the adaptor sequences were trimmed with Cutadapt (http://code.google.com/p/cutadapt/). Alignments against the mouse genome (mm10) and analysis of differential expressed genes were performed as previously described.[22] Cufflinks

software was used to calculate the number of fragments per kilobase of exon per million fragments mapped (FPKM) for each gene. FPKM values of *Sbds f/f* and +/+ recipients were then compared to the curated gene sets (C2) and the Gene Ontology gene sets (C5) of the Molecular Signature Database (MSigDB) by GSEA[23] (Broad Institute), using the Signal2Noise metric and 1000 phenotype-based permutations.

Statistical Analysis

Unless otherwise specified, statistical analysis was performed by an unpaired, 2-tailed Student's *t* test or 1-way analysis of variance. All results in bar graphs are reported as mean value ± standard error of the mean.

Results

Cebpa-driven deletion of *Sbds* in the hematopoietic system

To address the functional consequences of *Sbds* deficiency in early hematopoietic progenitors, we crossed *Sbds*-conditional knock-out mice, with loxP sites flanking the second exon of *Sbds*,[21] with *Cebpa*$^{cre/+}$ R26 EYFP mice[19] (Figure 1A). In this approach, Cre-mediated deletion of *Sbds* exon 2 in *Cebpa*-expressing cells results in a frameshift and consequently generates a premature stop codon, thus mimicking the effects of the 183-184TA→CT mutation in the human disease.[9] In addition, the R26 EYFP element enables the tracing of *Sbds*-depleted cells and their progeny based on enhanced yellow fluorescent protein (EYFP) expression.

Intercrossings of *Sbds*$^{f/+}$*;Cebpa*$^{cre/+}$*;R26*$^{EYFP/+}$ mice failed to generate any *Sbds*$^{f/f}$*;Cebpa*$^{cre/+}$ viable offspring (Online Supplementary Table S2). This, together with the small litter sizes, suggested that deficiency of *Sbds* in *Cebpa*-expressing cells is lethal in mice. Because *Cebpa* is expressed in non-hematopoietic tissues, like liver and lungs,[24] we analyzed E14.5 embryos from *Sbds*$^{f/+}$*;Cebpa*$^{cre/+}$ *R26*$^{EYFP/+}$ intercrosses to assess whether the lethal phenotype directly reflected hematopoietic dysfunction. Interestingly, at this

gestational age, *Sbds*$^{f/f}$;*Cebpa*$^{cre/+}$;*R26*$^{EYFP/+}$ (hereafter *Sbds f/f* or mutants) offspring was found at Mendelian frequencies (Online Supplementary Table S2) and these embryos were morphologically indistinguishable from their littermates. Genomic PCR indicated effective deletion of exon 2 in *Sbds f/f* embryos (Figure 1A, Figure 1B). We next compared hematopoiesis in *Sbds f/f* embryos with that of *Cebpa*$^{cre/+}$;*R26*$^{EYFP/+}$ controls (hence *Sbds* +/+) and found that *Sbds* recombination was associated with overall conservation of normal hematopoietic architecture in the fetal liver (Figure 1C). This suggests that embryonic lethality in this model is not caused by impaired blood cell production. The proportion of EYFP$^+$, Cre-targeted cells in each hematopoietic compartment was also similar in *Sbds f/f* and +/+ embryos, with the majority of GMPs and Gr1$^+$Mac1$^+$ mature granulocytes expressing EYFP (>90% and >60% of cells, respectively, Figure 1D). As expected,[19, 20] a small fraction of immunophenotypically defined HSCs, multipotent progenitors (MPPs), megakaryocyte-erythroid progenitors (MEPs) and B220$^+$ lymphocytes also expressed EYFP, indicating targeting of multilineage progenitors in this model.

Transplantation of *Sbds*-deleted fetal hematopoietic cells in adult mice results in neutropenia

To assess whether the deletion of *Sbds* in fetal hematopoietic progenitors would compromise postnatal hematopoiesis, we transplanted fetal liver cells from of E14.5 (CD45.2$^+$) *Sbds f/f* or +/+ embryos into lethally irradiated (CD45.1$^+$) B6.SJL mice (Figure 2A) and monitored hematopoiesis by peripheral blood analysis every 4 weeks. In both *Sbds f/f* and +/+ recipients more than 90% of circulating blood cells were CD45.2$^+$, indicating high chimerism in reconstituted mice. Mice transplanted with *Sbds*-deficient cells developed profound neutropenia, with an average 5.9-fold reduction of Gr1$^+$ Mac1$^+$ cells in the peripheral blood 5 weeks after transplantation (Figure 2B). Neutropenia was stable and persisted during the entire follow-up, i.e. 4 months after transplantation. Consistent with the hypothesis that loss of *Sbds* impairs myelopoiesis, the proportion of EYFP$^+$, Cre-targeted cells in *Sbds f/f* recipients (47.4±10.2%) was lower than that in controls (75.6±17.3%). In addition, numbers of circulating erythrocytes and B-cells were unaltered in steady state hematopoiesis after transplantation, while platelet numbers were increased in transplanted mice (Online Supplementary Figure S1).

Overall, the data indicates that *Sbds* is essential to maintain postnatal granulopoiesis and neutrophil homeostasis.

Sbds-deficiency in the myeloid lineage arrests differentiation at the myelocyte-metamyelocyte stage

To obtain insight into the cellular events caused by *Sbds* deficiency driving the defect in neutrophil development, we sacrificed mice 17 to 19 weeks after transplantation. *Cebpa* is expressed in myeloid progenitor cells and in a subpopulation of early progenitors that retain multilineage differentiation capacity.[19, 20] In line with this, EYFP expression was found in a small fraction of immunophenotypically defined hematopoietic stem and progenitor cells (HSPCs) and in all blood lineages ($Gr1^+Mac1^+$ myeloid, $Ter119^+$ erythroid and $B220^+$ lymphoid) at varying frequencies (Table 1; Figure 3A). The bone marrow of mice transplanted with *Sbds f/f* fetal liver cells was hypocellular, a common finding in SDS patients[7, 25] (Figure 3B). Hypocellularity resulted mostly from a marked reduction in $EYFP^+$ $Gr1^+$ $Mac1^+$ neutrophils (86 437 ± 33 601 cells per femur/body gram in *Sbds f/f* recipients and 316 442 ± 47 984 in controls), although also the number of $EYFP^+$ lymphoid and $Ter119^+$ erythroid cells was modestly decreased in mutant mice (Figure 3C, Figure 3D). Of note, myelodysplastic features were not observed in *Sbds f/f* recipients in the current model, suggesting that hematopoietic cell-extrinsic factors may contribute to myelodysplasia in SDS.[26]

Having established that *Sbds* deletion from multilineage hematopoietic progenitors results in neutropenia, we next sought to define the stages in myeloid lineage progression that were affected by loss of *Sbds*. It is generally assumed that loss of ribosome biogenesis genes affects rapidly proliferating progenitor cells with increased protein translation rates, although *in vivo* experimental support for this view has been lacking in the absence of a mammalian model of *Sbds* deficiency resulting in stable neutropenia. Efficient *Sbds* gene knockdown in $EYFP^+$ cells was first confirmed by quantitative RT-PCR throughout myeloid lineage development (Figure 3E), showing near complete deletion of *Sbds* expression at all stages of

myeloid development (LKS, CMP, GMP, immature and mature neutrophils). Interestingly, *Sbds* deficiency did not result in reduced numbers of hematopoietic progenitor cells along the myeloid lineage (Figure 3C, Figure 3D). Rather, a compensatory expansion of some progenitors was observed with numbers of both $EYFP^+$ and $EYFP^-$ GMPs dramatically increased in mice transplanted with *Sbds f/f* cells (average fold change, FC: 5.8 in $EYFP^+$ compartment and 5.9 in $EYFP^-$ cells; Figure 3D; Online Supplementary Figure S2), suggesting the emergence of reactive granulopoiesis in this cohort, defined as adaptation of the hematopoietic system to the increased demand through enhanced myeloid precursor cell proliferation in the bone marrow.[27]

We next aimed to further define the specific cell type in myeloid development that is critically dependent on *Sbds* function. FACS analysis revealed an increased frequency of c-Kit^{int} $Gr1^{low}$ cells, previously identified as myelocytes and metamyelocytes (MC-MMs, Figure 3F).[28] Both frequency and absolute count of more mature myeloid cells, characterized by loss of c-Kit expression and bright Gr1 staining, were lower, suggesting an arrest of lineage progression at the MC-MM stage. Morphological assessment of the bone marrow confirmed that terminal granulopoiesis is severely affected in *Sbds f/f* recipients, with accumulation of MC-MMs and reduced frequency of segmented neutrophils (Figure 3G; Online Supplementary Figure S3). Together, the data demonstrates that *Sbds* deletion from hematopoietic progenitor cells critically and specifically affects late stages of myeloid development, in particular the transition MC-MM to mature neutrophils.

Deficiency of *Sbds* deregulates myeloid differentiation programs and prevents cell-cycle-exit in myelocytes and metamyelocytes

To gain insight into the molecular programs associated with the proposed block of myeloid lineage progression at the MC-MM stage, the transcriptome of prospectively FACS-isolated $EYFP^+$ c-Kit^{int} $Gr1^{low}$ (MC-MM) cells was investigated by massive parallel RNA sequencing (RNA-Seq). As expected, *Sbds* expression in this population was significantly reduced in *Sbds f/f* recipients ($\log_2$ FC = -2.39, False

Discovery Rate, FDR=6.6x10^{-9}, Figure 4A). Consistent with its postulated function in ribosome biogenesis, *Sbds* deficiency significantly (FDR<0.25) affected transcriptional signatures related to translation and ribosome biogenesis (Figure 4B; Online Supplementary Table S3 and S4).

Gene set enrichment analysis (GSEA) highlighted the enrichment of relatively immature hematopoietic signatures in *Sbds f/f* MC-MMs, whereas data sets associated with cell differentiation were enriched in controls, consistent with a defect in maturation (Figure 4C; Online Supplementary Table S3). To specifically define the stage in which myeloid differentiation is impaired, we examined the expression of transcripts encoding constituents of myeloid granules. In myeloid development, primary granules are produced in promyelocytes, whereas secondary granule production starts in myelocytes and gelatinase-containing tertiary granules become apparent in metamyelocytes and in band cells.[29, 30] Transcript analysis showed significantly reduced expression of secondary and tertiary granule components, whereas transcripts encoding constituents of primary granules were significantly enriched, indicating that development is specifically arrested in myelocytes, consistent with flow-cytometric findings (Figure 4D).

To definitively establish the myelocyte as the cell type in the myeloid lineage critically depending on *Sbds* expression, we next performed cell cycle analysis. Myelocytes represent the last cell in myeloid differentiation capable of mitotic division[31] and cell cycle exit is a required process for terminal granulopoiesis[32]. Ki67 analysis by FACS demonstrated that c-Kit^{int} $Gr1^{low}$ cells indeed failed to exit the cell cycle, congruent with the notion that *Sbds* deficiency attenuates lineage progression in myelocytes (Figure 4E, Figure 4F). Molecularly, this failure to exit the cell cycle was associated with significant reduced expression of the transcription factor retinoic acid receptor α (RARα) and its downstream transcriptional targets *Itgb2* and p27 (*Cdkn1b*),[33, 34] key activators of the terminal myeloid differentiation program and cell cycle exit (Figure 4G). Together, the data demonstrates that loss of *Sbds* from hematopoietic progenitors results in failure of lineage progression specifically in myelocytes, which is associated with attenuation of myeloid differentiation signatures and cellular events.

Loss of *Sbds* results in activation of the p53 tumor suppressor pathway and apoptosis in late stage myeloid cells

Finally, we shought to better define the underlying cellular and molecular mechanisms of the arrest in lineage progression at the stage of myelocytes. Activation of p53 has been proposed as a common mechanism in the pathogenesis of different ribosomopathies, including DBA, Treacher Collins syndrome and 5q- syndrome[35]. In SDS, overexpression of p53 in immature cells has been described in bone marrow biopsies from SDS patients[36] but the consequences of p53 activation for disease pathogenesis have not been experimentally defined. Transcriptional activation of the p53 pathway was observed in *Sbds f/f* MC-MMs by GSEA analysis (Figure 5A). Specifically, RNA sequencing demonstrated a significant increase in transcripts for p53 itself and many of its downstream targets, including the cell cycle regulators *Cdkn1a* (p21) and *Zmat3* (Wig1) and the pro-apoptotic genes *Bbc3* (PUMA), *Bax*, *Tnfrsf10b* (Death Receptor 5) and *Cycs* (cytochrome c, somatic) (Figure 5B). FACS analysis confirmed intracellular accumulation of the p53 protein, specifically at late stages of myelopoiesis (MC-MM and c-Kit $^{-}$ EYFP+ populations) in *Sbds f/f* recipients (FC = 1.78 and 1.53, respectively, Figure 5C). In line with this activation of the p53 tumor suppressor pathway and increased expression of pro-apoptotic genes, an increased rate of apoptosis (annexin V^{+} $7AAD^{-}$ cells) was found in p53-overexpressing c-Kit^{int} and c-Kit^{-} $EYFP^{+}$ populations (Figure 5D). Of note, no significant p53 accumulation or apoptosis was observed in more immature progenitors ($cKit^{+}$ $EYFP^{+}$ cells).

Collectively, the findings indicate that *Sbds* deficiency in the myeloid lineage specifically attenuates lineage progression at the myelocyte stage through activation of cellular stress pathways and induction of p53-associated apoptosis.

Discussion

Neutropenia is the principal hematological manifestation of SDS, but the cellular and molecular mechanisms underlying this specific disease phenotype remain poorly understood. Here, we established a

mammalian model of *Sbds* deficiency-induced neutropenia, revealing a critical dependency of myelocytes and their downstream progeny on the function of this ribosomal biogenesis gene through induction of p53-associated apoptosis, thus providing a cellular and molecular basis for the understanding of neutropenia in this disease.

Several findings in our study point towards myelocytes as the differentiation stage critically impaired by *Sbds* deficiency. First, the data indicates that myelocytes accumulate in *Cebpa*-cre *Sbds* mutant mice and fail to exit the cell cycle, a process typically occurring at the myelocyte stage and required for terminal differentiation towards mature neutrophils.[31, 32] Secondly, massive parallel transcriptional profiling of prospectively isolated MC-MMs revealed specifically reduced expression of genes encoding constituents of secondary and tertiary granule proteins, the production of which specifically marks the transition from promyelocytes to myelocytes in myeloid development.[29, 30] Finally, *Sbds* deficiency in myelocytes was associated with reduced expression of the myeloid transcription factor RARα and its downstream transcriptional targets. RARα is an important regulator of myelopoiesis with a putative role in terminal granulocyte differentiation.[37] *In vitro* differentiation studies show that RAR deficiency blocks lineage progression at the myelocyte stage[38] and *in vivo* inhibition of endogenous retinoids results in accumulation of immature myeloid cells in wild type mice.[37]

While *Sbds* deletion in the myeloid lineage specifically attenuated lineage progression downstream of myelocytes, deficiency of *Sbds* did not functionally affect rapidly cycling hematopoietic progenitor cells (HPCs). This finding was initially unanticipated since HPCs are thought to have a relatively high rate of protein synthesis in comparison to HSCs and other cells of the hematopoietic hierarchy[39] and it seemed therefore reasonable to predict that rapidly cycling progenitors are more sensitive to defects of ribosome biogenesis and protein translation. In line with this view, reduced frequency or altered activity of HPCs have been previously suggested to drive cytopenia in both DBA and SDS,[40-42] albeit this does not provide a satisfactory explanation for lineage specificity in these diseases. In our model, the efficacy of *Sbds* deletion was comparable throughout myeloid development (*Cebpa*-expressing LKS, CMP, GMP and the

myelocyte compartment), yet the size of the progenitor pool in the bone marrow increased, while the number of mature neutrophils was reduced. This finding seems congruent with observations in zebrafish, where deletion of *Sbds* induces loss of neutrophils, but does not affect spi1 (PU.1) positive progenitors.[43]

The resulting left-shifted myelopoiesis in our model is reminiscent of that observed *in vitro* upon granulocytic differentiation of *Sbds*-knockdown hematopoietic cells, resulting in an accumulation of MC-MMs,[17] and of the maturation defect that characterizes a subset of SDS patients.[5, 7, 25, 44] While our findings provide a basis for understanding the myeloid lineage specificity of ribosomal dysfunction in SDS, in translating these findings to human disease it is important to point out that pluripotent hematopoietic stem cells are incompletely targeted in this model. *Cebpa*-driven deletion of *Sbds* occurred in a small subset of immunophenotypically defined, multipotent HSCs, reflected in a modest decrease in erythroid and lymphoid cells in the EYFP+ compartment of mutant mice. It is therefore reasonable to assume that *Sbds* deficiency in the hematopoietic system does not exclusively, but rather predominantly, affects the myeloid lineage. It is conceivable that in human disease composite effects of *Sbds* deficiency in pluripotent HSCs, potentially reducing numbers of (normally functioning) hematopoietic progenitor cells,[42, 44, 45] synergize with a specific impairment of lineage progression in late myeloid differentiation phases to impair granulopoiesis. Incomplete HSC targeting may also explain the apparent absence of homing defects, previously reported in a transplant model of *Sbds* downregulation in HSC.[17] This notion may help understand why we have been able to establish a stable model of neutropenia, where incomplete targeting of HSCs allowed durable and robust engraftment of hematopoiesis enabling the detailed analysis of long-term myeloid lineage progression in mutant mice.

Identification of the cells driving neutropenia within the *Sbds*-deficient hematopoietic hierarchy allowed us to begin defining the cellular and molecular events underlying neutropenia in SDS. Our study describes activation of the p53 pathway and an associated increase in apoptotic rates specifically in myelocytes and their downstream progeny. The data seems congruent with observations in human disease where an intrinsic propensity for apoptosis is seen in hematopoietic cells after 7-day culture of CD34+ cells in

medium containing G-CSF[46] with a lack of correlation between colony numbers and apoptosis rate, indicating that the number of CFU-C is not affected in SDS patients. Activation of the p53 pathway has been suggested to represent a molecular commonality in ribosomopathies and perhaps congenital neutropenias[47] but experimental support for this view in SDS has been lacking. Our findings do not, however, exclude the possibility that other mechanisms are involved in the failure in cell cycle progression and neutropenia in SDS.

It is conceivable that the loss of function of *Sbds* affects the translation of specific transcription factors driving terminal myeloid differentiation, including those upstream of RARα. In particular, the mRNA of specific transcription factor isoforms may be characterized by distinct 5'-UTRs, some of them predicted to have a complex secondary structure.[48] These complex 5'-UTRs are typically associated with high demands for translation initiation factors and may thus confer particular sensitivity to conditions of translational stress. Such a mechanism of reduced translation efficiency has recently been shown to affect GATA1 protein levels in the pathogenesis of DBA.[49] Alternatively, the high and specific demand of protein synthesis and cotranslational assembly into secretory granules, which characterizes and defines myelocytes and their downstream progeny, may cause specific translational stress, resulting in activation of cellular alarm pathways and downstream events including impaired differentiation. In this context, it is interesting to note previous observations in induced pluripotent stem cell models of SDS, indicating granule abnormalities in pancreatic and myeloid cells,[50] and in a mouse model of pancreatic-specific *Sbds* deficiency, showing reduced *in vivo* zymogen granule formation in acinar cells,[21] perhaps pointing towards impaired secretory granule maturation as a common mechanism underlying tissue specificity in SDS.[50] Our current model will allow the interrogation of these potential mechanisms which is ultimately anticipated to result in novel, targeted therapeutic strategies for SDS.

Disclosures

The authors report no potential conflicts of interest.

References

1. Shwachman H, Diamond LK, Oski FA, Khaw KT. The Syndrome of Pancreatic Insufficiency and Bone Marrow Dysfunction. J Pediatr. 1964;65:645-663.

2. Huang JN, Shimamura A. Clinical spectrum and molecular pathophysiology of Shwachman-Diamond syndrome. Curr Opin Hematol. 2011;18(1):30-35.

3. Tamary H, Alter BP. Current diagnosis of inherited bone marrow failure syndromes. Pediatr Hematol Oncol. 2007;24(2):87-99.

4. Mack DR, Forstner GG, Wilschanski M, Freedman MH, Durie PR. Shwachman syndrome: Exocrine pancreatic dysfunction and variable phenotypic expression. Gastroenterology. 1996;111(6):1593-1602.

5. Ginzberg H, Shin J, Ellis L, et al. Shwachman syndrome: phenotypic manifestations of sibling sets and isolated cases in a large patient cohort are similar. J Pediatr. 1999;135(1):81-88.

6. Dror Y. Shwachman-Diamond syndrome. Pediatr Blood Cancer. 2005;45(7):892-901.

7. Donadieu J, Fenneteau O, Beaupain B, et al. Classification of and risk factors for hematologic complications in a French national cohort of 102 patients with Shwachman-Diamond syndrome. Haematologica. 2012;97(9):1312-1319.

8. Myers KC, Bolyard AA, Otto B, et al. Variable Clinical Presentation of Shwachman-Diamond Syndrome: Update from the North American Shwachman-Diamond Syndrome Registry. J Pediatr. 2014;164(4):866-870.

9. Boocock GR, Morrison JA, Popovic M, et al. Mutations in SBDS are associated with Shwachman-Diamond syndrome. Nat Genet. 2003;33(1):97-101.

10. Finch AJ, Hilcenko C, Basse N, et al. Uncoupling of GTP hydrolysis from eIF6 release on the ribosome causes Shwachman-Diamond syndrome. Gene Dev. 2011;25(9):917-929.

11. Menne TF, Goyenechea B, Sanchez-Puig N, et al. The Shwachman-Bodian-Diamond syndrome protein mediates translational activation of ribosomes in yeast. Nat Genet. 2007;39(4):486-495.

12. Wong CC, Traynor D, Basse N, Kay RR, Warren AJ. Defective ribosome assembly in Shwachman-Diamond syndrome. Blood. 2011;118(16):4305-4312.

13. Burwick N, Coats SA, Nakamura T, Shimamura A. Impaired ribosomal subunit association in Shwachman-Diamond syndrome. Blood. 2012;120(26):5143-5152.

14. De Keersmaecker K, Sulima SO, Dinman JD. Ribosomopathies and the paradox of cellular hypo- to hyperproliferation. Blood. 2015;125(9):1377-1382.

15. Ruggero D, Shimamura A. Marrow failure: a window into ribosome biology. Blood. 2014;124(18):2784-2792.

16. Zhang S, Shi M, Hui CC, Rommens JM. Loss of the mouse ortholog of the shwachman-diamond syndrome gene (Sbds) results in early embryonic lethality. Mol Cell Biol. 2006;26(17):6656-6663.

17. Rawls AS, Gregory AD, Woloszynek JR, Liu FL, Link DC. Lentiviral-mediated RNAi inhibition of Sbds in murine hematopoietic progenitors impairs their hematopoietic potential. Blood. 2007;110(7):2414-2422.

18. Zhang P, Iwasaki-Arai J, Iwasaki H, et al. Enhancement of hematopoietic stem cell repopulating capacity and self-renewal in the absence of the transcription factor C/EBP alpha. Immunity. 2004;21(6):853-863.

19. Wölfler A, Oorschot AADV, Haanstra JR, et al. Lineage-instructive function of C/EBP alpha in multipotent hematopoietic cells and early thymic progenitors. Blood. 2010;116(20):4116-4125.

20. Ye M, Zhang H, Amabile G, et al. C/EBPa controls acquisition and maintenance of adult haematopoietic stem cell quiescence. Nat Cell Biol. 2013;15(4):385-394.

21. Tourlakis ME, Zhong J, Gandhi R, et al. Deficiency of Sbds in the Mouse Pancreas Leads to Features of Shwachman-Diamond Syndrome, With Loss of Zymogen Granules. Gastroenterology. 2012;143(2):481-492.

22. Gröschel S, Sanders MA, Hoogenboezem R, et al. A Single Oncogenic Enhancer Rearrangement Causes Concomitant EVI1 and GATA2 Deregulation in Leukemia. Cell. 2014;157(2):369-381.

23. Subramanian A, Tamayo P, Mootha VK, et al. Gene set enrichment analysis: a knowledge-based approach for interpreting genome-wide expression profiles. Proc Natl Acad Sci U S A. 2005;102(43):15545-15550.

24. Flodby P, Barlow C, Kylefjord H, Ahrlund-Richter L, Xanthopoulos KG. Increased hepatic cell proliferation and lung abnormalities in mice deficient in CCAAT/enhancer binding protein alpha. J Biol Chem. 1996;271(40):24753-24760.

25. Aggett PJ, Cavanagh NPC, Matthew DJ, Pincott JR, Sutcliffe J, Harries JT. Shwachman's Syndrome. A Review of 21 Cases. Arch Dis Child. 1980;55(5):331-347.

26. Raaijmakers MH, Mukherjee S, Guo S, et al. Bone progenitor dysfunction induces myelodysplasia and secondary leukaemia. Nature. 2010;464(7290):852-857.

27. Manz MG, Boettcher S. Emergency granulopoiesis. Nat Rev Immunol. 2014;14(5):302-314.

28. Satake S, Hirai H, Hayashi Y, et al. C/EBP beta Is Involved in the Amplification of Early Granulocyte Precursors during Candidemia-Induced "Emergency" Granulopoiesis. J Immunol. 2012;189(9):4546-4555.

29. Borregaard N, Sehested M, Nielsen BS, Sengelov H, Kjeldsen L. Biosynthesis of Granule Proteins in Normal Human Bone-Marrow Cells. Gelatinase Is a Marker of Terminal Neutrophil Differentiation. Blood. 1995;85(3):812-817.

30. Borregaard N, Cowland JB. Granules of the human neutrophilic polymorphonuclear leukocyte. Blood. 1997;89(10):3503-3521.

31. Bainton DF, Ullyot JL, Farquhar MG. The development of neutrophilic polymorphonuclear leukocytes in human bone marrow. J Exp Med. 1971;134(4):907-934.

32. Wang QF, Cleaves R, Kummalue T, Nerlov C, Friedman AD. Cell cycle inhibition mediated by the outer surface of the C/EBPalpha basic region is required but not sufficient for granulopoiesis. Oncogene. 2003;22(17):2548-2557.

33. Walkley CR, Purton LE, Snelling HJ, et al. Identification of the molecular requirements for an RAR alpha-mediated cell cycle arrest during granulocytic differentiation. Blood. 2004;103(4):1286-1295.

34. Bush TS, St Coeur M, Resendes KK, Rosmarin AG. GA-binding protein (GABP) and Sp1 are required, along with retinoid receptors, to mediate retinoic acid responsiveness of CD18 (beta 2 leukocyte integrin): a novel mechanism of transcriptional regulation in myeloid cells. Blood. 2003;101(1):311-317.

35. Fumagalli S, Thomas G. The role of p53 in ribosomopathies. Semin Hematol. 2011;48(2):97-105.

36. Elghetany MT, Alter BP. p53 protein overexpression in bone marrow biopsies of patients with Shwachman-Diamond syndrome has a prevalence similar to that of patients with refractory anemia. Arch Pathol Lab Med. 2002;126(4):452-455.

37. Kastner P, Lawrence HJ, Waltzinger C, Ghyselinck NB, Chambon P, Chan S. Positive and negative regulation of granulopoiesis by endogenous RARalpha. Blood. 2001;97(5):1314-1320.

38. Labrecque J, Allan D, Chambon P, Iscove NN, Lohnes D, Hoang T. Impaired granulocytic differentiation in vitro in hematopoietic cells lacking retinoic acid receptors alpha1 and gamma. Blood. 1998;92(2):607-615.

39. Signer RAJ, Magee JA, Salic A, Morrison SJ. Haematopoietic stem cells require a highly regulated protein synthesis rate. Nature. 2014;509(7498):49-54.

40. Perdahl EB, Naprstek BL, Wallace WC, Lipton JM. Erythroid Failure in Diamond-Blackfan Anemia Is Characterized by Apoptosis. Blood. 1994;83(3):645-650.

41. Dutt S, Narla A, Lin K, et al. Haploinsufficiency for ribosomal protein genes causes selective activation of p53 in human erythroid progenitor cells. Blood. 2011;117(9):2567-2576.

42. Dror Y, Freedman MH. Shwachman-Diamond syndrome: An inherited preleukemic bone marrow failure disorder with aberrant hematopoietic progenitors and faulty marrow microenvironment. Blood. 1999;94(9):3048-3054.

43. Provost E, Wehner KA, Zhong XG, et al. Ribosomal biogenesis genes play an essential and p53-independent role in zebrafish pancreas development. Development. 2012;139(17):3232-3241.

44. Mercuri A, Cannata E, Perbellini O, et al. Immunophenotypic Analysis of Hematopoiesis in Patients suffering from Shwachman-Bodian-Diamond Syndrome. Eur J Haematol 2014 Nov 17. [Epub ahead of print]

45. Saunders EF, Gall G, Freedman MH. Granulopoiesis in Shwachman's syndrome (pancreatic insufficiency and bone marrow dysfunction). Pediatrics. 1979;64(4):515-519.

46. Dror Y, Freedman MH. Shwachman-Diamond syndrome marrow cells show abnormally increased apoptosis mediated through the Fas pathway. Blood. 2001;97(10):3011-3016.

47. Glaubach T, Minella AC, Corey SJ. Cellular stress pathways in pediatric bone marrow failure syndromes: many roads lead to neutropenia. Pediatr Res. 2014;75(1-2):189-195.

48. Yost CC, Denis MM, Lindemann S, et al. Activated polymorphonuclear leukocytes rapidly synthesize retinoic acid receptor-alpha: a mechanism for translational control of transcriptional events. J Exp Med. 2004;200(5):671-680.

49. Ludwig LS, Gazda HT, Eng JC, et al. Altered translation of GATA1 in Diamond-Blackfan anemia. Nat Med. 2014;20(7):748-753.

50. Tulpule A, Kelley JM, Lensch MW, et al. Pluripotent stem cell models of Shwachman-Diamond syndrome reveal a common mechanism for pancreatic and hematopoietic dysfunction. Cell Stem Cell. 2013;12(6):727-736.

Table 1. Frequency of EYFP+ cells within hematopoietic subsets in the bone marrow.

	Sbds +/+ [a]	*Sbds f/f* [a]
LKS[b]	3.3% (1.61% - 5.82%)	7.4% (1.67% - 11.5%)
CMP[b]	31.2% (24.0% - 41.6%)	22.5% (16.3% - 31.6%)
MEP[b]	8.2% (6.3% - 10.2%)	5.8% (4.92% - 6.79%)
GMP[b]	72.3% (63.7% - 77.6%)	67.7% (62.6% - 72.3%)
$Gr1^+$ $Mac1^+$ [c]	87.9% (86.2% - 89.1%)	76.1% (74.3% - 77.7%)
$B220^+$ [c]	8.8% (5.4% - 13.2%)	4.4% (3.3% - 5.9%)
$Ter119^+$ [d]	3.0% (2.2% - 4.1%)	1.8% (0.7% - 3.2%)

[a] The percentage of $EYFP^+$ cells in different hematopoietic populations is indicated as mean frequency (range). [b] n = 7. [c] *Sbds* +/+, n = 7; *Sbds f/f*, n=6. [d] *Sbds* +/+, n = 5; *Sbds f/f*, n = 4.

Figure legends

Figure 1. *Sbds*-deletion from myeloid progenitor cells does not perturb the architecture of fetal liver hematopoiesis.

(A) Schematic representation of the targeting vectors and the primers used in the study. Primer sequences are listed in Online Supplementary Table 1. (B) Genomic analysis of E14.5 embryos confirmed excision of *Sbds* in f/f mice. a + b, genotyping primers. c + d, deletion primers. (C-D) Normal composition of fetal liver (*Sbds* +/+, *n* = 4; *Sbds f/f*, *n* = 6). (C) Frequency of hematopoietic subsets in live cells (7AAD-). (D) Proportion of $EYFP^+$ cells in each hematopoietic population. Data is mean ± s.e.m. Differences between *Sbds* +/+ and *f/f* mice are not significant. HSC, Lin^- $c\text{-}Kit^+$ $Sca1^+$ (LKS) $CD48^-$ $CD150^+$ cells. Multipotent progenitors (MPP), LKS $CD48^-$ $CD150^-$ cells. Common myeloid progenitor (CMP), Lin^- $c\text{-}Kit^+$ $Sca1^-$ $CD34^+$ $CD16/32^-$ cells. Granulocyte-macrophage progenitor (GMP), Lin^- $c\text{-}Kit^+$ $Sca1^-$ $CD34^+$ $CD16/32^+$ cells.

Figure 2. Loss of *Sbds* from C/EBPα-expressing cells causes neutropenia in mice.

(A) Experimental design. 300 000 fetal liver cells from either *Sbds* +/+ or *f/f* embryos (E14.5) were transplanted into 7 to 10-week-old lethally irradiated $CD45.1^+$ B6.SJL mice (*n* = 7 per group). (B) Peripheral blood analysis at 5 and 16 weeks after transplantation showed severe reduction of granulocytes ($Gr1^+$ $Mac1^+$ cells) upon *Sbds* deletion. Each circle represents one mouse. The horizontal line depicts average values. WBC, white blood cells. ** $P < 0.01$, ***$P < 0.001$.

Figure 3. *Sbds*-deficiency in hematopoiesis attenuates myeloid lineage progression at the myelocyte-metamyelocyte stage.

(A) Donut chart illustrating the percentage of different hematopoietic subsets within the $EYFP^+$ compartment in the bone marrow of *Sbds* +/+ and *f/f* recipients. (B) Decreased cellularity upon transplantation of *Sbds*-deficient cells. (C-D) Absolute number of $EYFP^+$ cells in different hematopoietic populations in the bone marrow (*Sbds* +/+, *n* = 7*; Sbds f/f*, *n* = 6, data is mean ± s.e.m). (C) LKS subsets.

(D) Reduction of EYFP$^+$ mature granulocytes in *Sbds f/f*-transplanted mice is associated with an increase of granulocyte-macrophage progenitors. (E) Deletion efficacy. Expression of *Sbds* is reduced in LKS and throughout the myeloid differentiation stages in *Sbds f/f* EYFP$^+$ cells. (F) Loss of late myeloid cells in *Sbds f/f* mice. Upper panel, representative plots of EYFP$^+$ cells. Lower panel, percentage of c-Kit$^+$ Gr1$^-$ myeloblasts and promyelocytes (i), c-Kit^{int} Gr1^{low} myelocytes and metamyelocytes (ii) and c-Kit$^-$ Gr1$^+$ band and segmented cells (iii) in EYFP$^+$ cells from *Sbds* +/+ and *f/f* cohorts. (G) Accumulation of myelocytes and metamyelocytes (black arrows) in *Sbds*-deficient bone marrow (original magnification x63). * $P < 0.05$, ** $P < 0.01$, ***$P < 0.001$.

Figure 4. *Sbds* deficiency results in failure of cell cycle exit and secondary granule formation in myelopoiesis.

(A) Expression of *Sbds* in c-Kit^{int} Gr1^{low} EYFP$^+$ cells by RNA-Seq ($n = 4$). Each circle represents one mouse. (B-C) GSEA plots showing enrichment of data sets relating to translation (B) and immature hematopoietic features (Ci) in c-Kit^{int} Gr1^{low} EYFP$^+$ cells from *Sbds f/f* recipients and enrichment of maturation signatures in the *Sbds* +/+ group (Cii). Genes in the datasets are represented by black bars distributed according to their differential expression between *Sbds f/f* and *Sbds* +/+ cohorts. NES: Normalized Enrichment Score. (D) Reduced expression of genes encoding secondary and tertiary granule proteins in *Sbds f/f* c-Kit^{int} Gr1^{low} EYFP$^+$ cells with enrichment of transcripts encoding primary granules components. (E-F) *Sbds* deficiency impairs cell cycle exit in myelopoiesis (*Sbds* +/+, $n = 5$; *Sbds f/f*, $n = 4$). (E) Gating strategy in representative FACS plots. (F) Percentage of cells in G0 (Ki67$^-$ 7AAD^{low}), G1 (Ki67$^+$ 7AAD^{low}) and S-G2-M (Ki67$^+$ 7AAD^{high}) in each YFP$^+$ population. (G) Downregulation of *Rara*, *Cdkn1b* (p27) and *Itgb2* in recipients of *Sbds*-deficient cells ($n = 4$). Data is mean ± s.e.m. * $P < 0.05$, ** $P < 0.01$, ***$P < 0.001$. † $FDR < 0.05$, †† $FDR < 0.01$, †††$FDR < 0.001$.

Figure 5. Activation of p53 and apoptosis in late stages of *Sbds*-deficient myeloid development.

(A) Enrichment of p53 signatures in the transcriptome of MC-MMs from *Sbds f/f* recipients ($n = 4$). (B) Increased transcript levels of *Trp53* and its downstream transcriptional targets in RNA-Seq data. (C) Accumulation of p53 protein in late stages of myelopoiesis. Ci, representative histograms. Cii, mean fluorescence intensities in different EYFP+ populations (*Sbds* +/+, $n = 5$; *Sbds f/f*, $n = 4$). (D) Increased rates of apoptosis in late myeloid cells upon *Sbds* deletion ($n = 4$). Left, representative plot. Right, frequency of annexin V+ 7AAD- apoptotic cells in different stages of myelopoiesis. Data in bar graphs is mean ± s.e.m. $^{*}P < 0.05$, $^{***}P < 0.001$. †FDR < 0.05, †††FDR < 0.001.

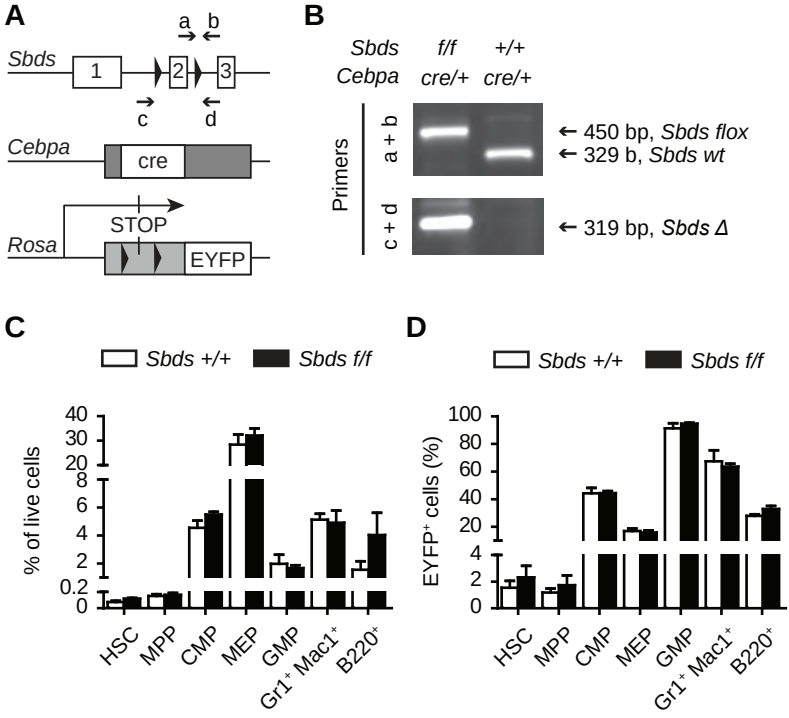
A
a
b
Sbds
1
2
3
c
d
Cebpa
cre
STOP
Rosa
EYFP
B
Sbds f/f +/+
Cebpa cre/+ cre/+
Primers
a + b
c + d
← 450 bp, Sbds flox
← 329 b, Sbds wt
← 319 bp, Sbds Δ
C
Sbds +/+
Sbds f/f
% of live cells
40
30
20
8
6
4
2
0.2
0
HSC
MPP
CMP
MEP
GMP
Gr1+ Mac1+
B220+
D
Sbds +/+
Sbds f/f
EYFP+ cells (%)
100
80
60
40
20
4
2
0
HSC
MPP
CMP
MEP
GMP
Gr1+ Mac1+
B220+

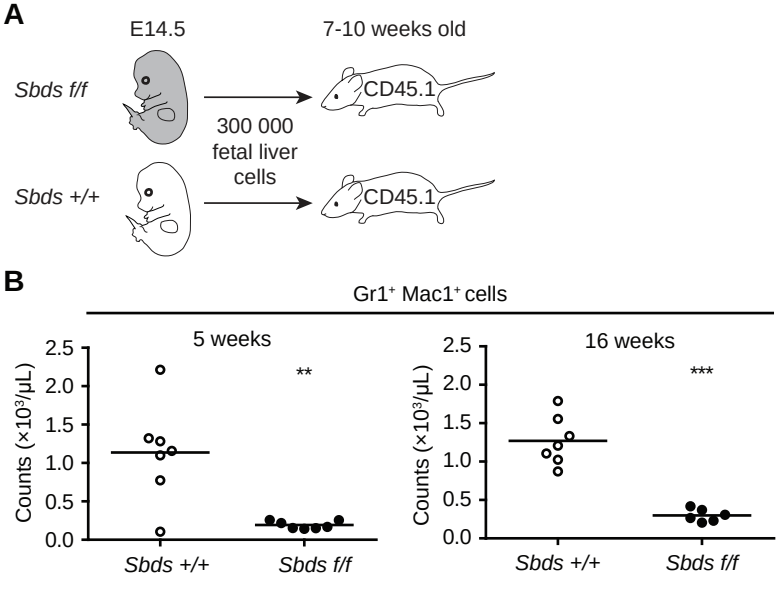
A
E14.5
7-10 weeks old
Sbds f/f
CD45.1
300 000
fetal liver
cells
Sbds +/+
CD45.1
B
Gr1+ Mac1+ cells
5 weeks
16 weeks
Counts (×10³/μL)
2.5
2.0
1.5
1.0
0.5
0.0
**
***
Sbds +/+
Sbds f/f

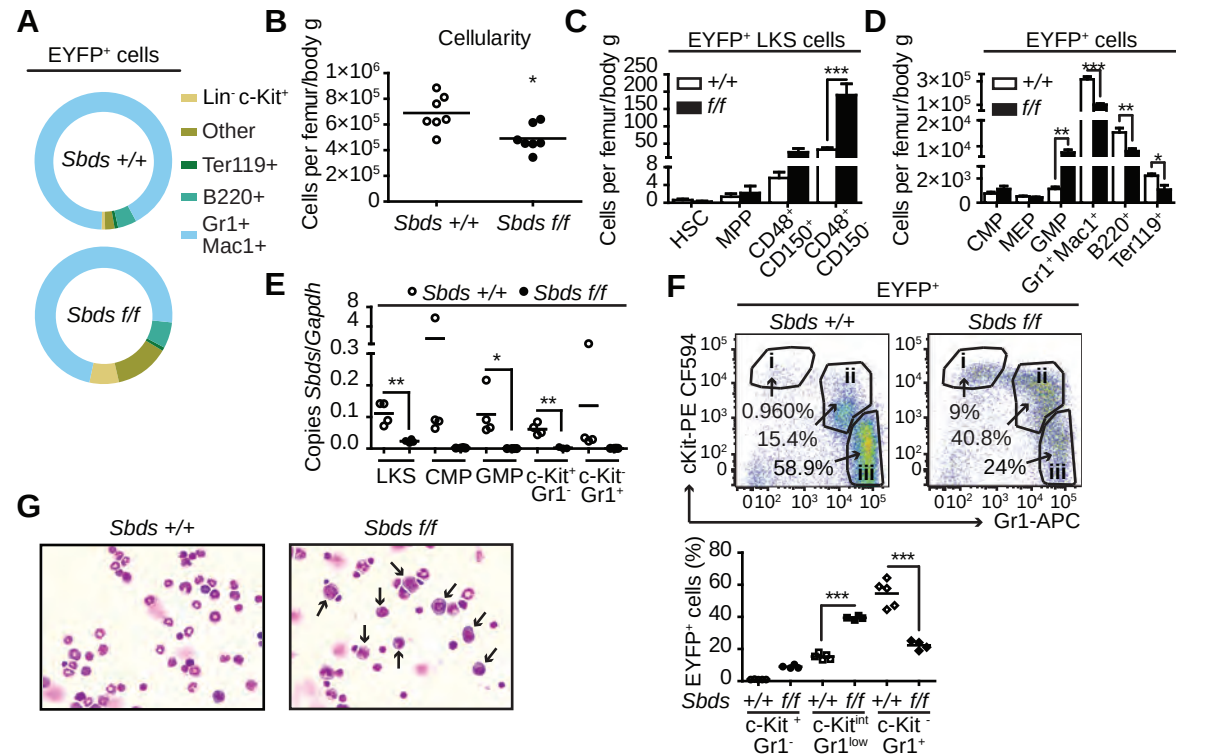
A
EYFP+ cells
Sbds +/+
Sbds f/f
Lin- c-Kit+
Other
Ter119+
B220+
Gr1+ Mac1+
B
Cellularity
Cells per femur/body g
1×10^6
8×10^5
6×10^5
4×10^5
2×10^5
0
Sbds +/+
Sbds f/f
C
EYFP+ LKS cells
Cells per femur/body g
250
200
150
100
50
8
4
0
+/+
f/f
HSC
MPP
CD48+ CD150+
CD48+ CD150-
D
EYFP+ cells
Cells per femur/body g
3×10^5
1×10^5
2×10^4
1×10^4
2×10^3
0
CMP
MEP
GMP
Gr1+Mac1+
B220+
Ter119+
E
Sbds +/+
Sbds f/f
Copies Sbds/Gapdh
8
4
0.3
0.2
0.1
0.0
LKS
CMP
GMP
c-Kit+ Gr1-
c-Kit- Gr1+
F
EYFP+
Sbds +/+
Sbds f/f
cKit-PE CF594
Gr1-APC
0.960%
15.4%
58.9%
9%
40.8%
24%
EYFP+ cells (%)
Sbds
c-Kit + Gr1-
c-Kit int Gr1low
c-Kit - Gr1+
G
Sbds +/+
Sbds f/f

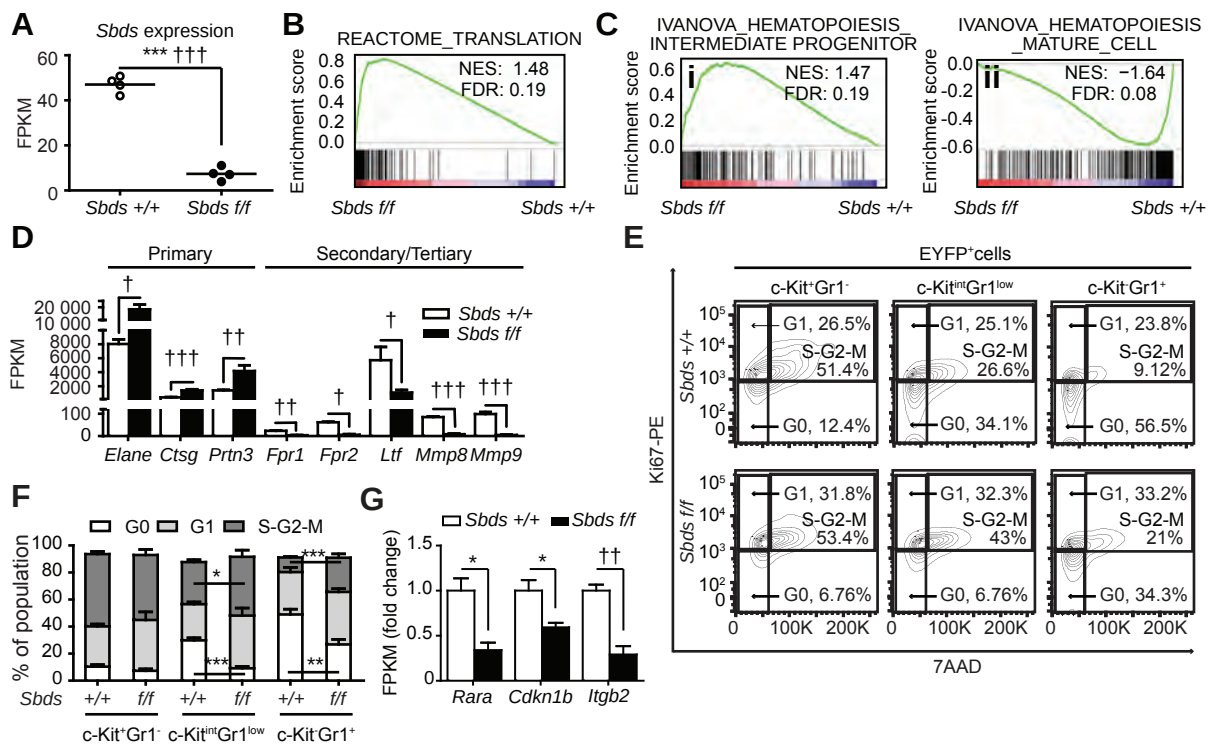
A
Sbds expression
*** †††
FPKM
60
40
20
0
Sbds +/+
Sbds f/f
B
REACTOME_TRANSLATION
Enrichment score
0.8
0.6
0.4
0.2
0.0
NES: 1.48
FDR: 0.19
Sbds f/f
Sbds +/+
C
IVANOVA_HEMATOPOIESIS_ INTERMEDIATE PROGENITOR
i
NES: 1.47
FDR: 0.19
IVANOVA_HEMATOPOIESIS _MATURE_CELL
ii
NES: −1.64
FDR: 0.08
D
Primary
Secondary/Tertiary
FPKM
20 000
10 000
8000
6000
4000
2000
100
0
Sbds +/+
Sbds f/f
Elane
Ctsg
Prtn3
Fpr1
Fpr2
Ltf
Mmp8
Mmp9
E
EYFP+cells
c-Kit+Gr1-
c-Kitintgr1low
c-Kit-Gr1+
Sbds +/+
Sbds f/f
G1, 26.5%
S-G2-M 51.4%
G0, 12.4%
G1, 25.1%
S-G2-M 26.6%
G0, 34.1%
G1, 23.8%
S-G2-M 9.12%
G0, 56.5%
G1, 31.8%
S-G2-M 53.4%
G0, 6.76%
G1, 32.3%
S-G2-M 43%
G0, 6.76%
G1, 33.2%
S-G2-M 21%
G0, 34.3%
Ki67-PE
7AAD
0
100K
200K
F
G0
G1
S-G2-M
% of population
Sbds
+/+
f/f
c-Kit+Gr1-
c-Kitintgr1low
c-Kit-Gr1+
G
Sbds +/+
Sbds f/f
FPKM (fold change)
1.5
1.0
0.5
Rara
Cdkn1b
Itgb2

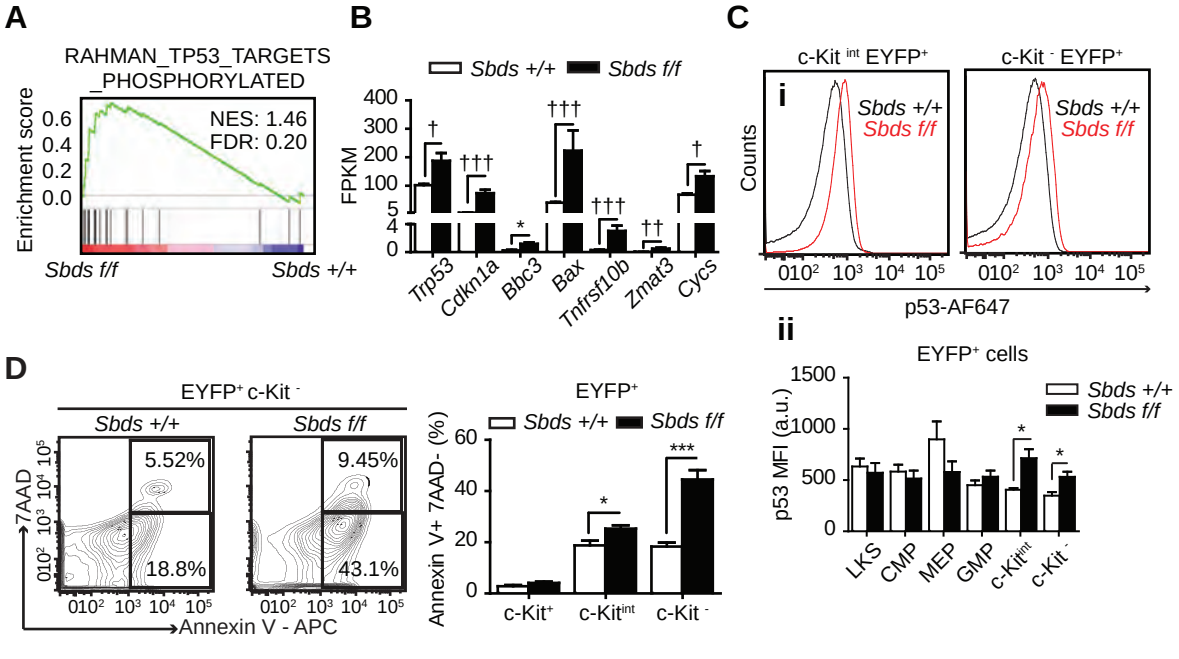
A
RAHMAN_TP53_TARGETS
_PHOSPHORYLATED
Enrichment score
NES: 1.46
FDR: 0.20
Sbds f/f
Sbds +/+
B
Sbds +/+
Sbds f/f
FPKM
Trp53
Cdkn1a
Bbc3
Bax
Tnfrsf10b
Zmat3
Cycs
C
c-Kit int EYFP+
c-Kit - EYFP+
i
Counts
p53-AF647
ii
EYFP+ cells
p53 MFI (a.u.)
LKS
CMP
MEP
GMP
c-Kitint
c-Kit -
D
EYFP+ c-Kit -
5.52%
18.8%
9.45%
43.1%
7AAD
Annexin V - APC
EYFP+
Annexin V+ 7AAD- (%)
c-Kit+
c-Kitint
c-Kit -

Supplementary methods, tables and figures

Supplemental methods

Peripheral Blood Measurements

Peripheral blood was collected by submandibular bleeding in K2EDTA-coated microtainers (BD). Hematological parameters were analyzed using a Vet ABC counter (Scil Animal Care).

Flow Cytometry

Bone marrow cells were isolated as previously reported.[1] Red blood cells (RBC) from bone marrow and fetal liver were lysed with ACK lysing buffer (Lonza) before FACS staining. Peripheral blood cells were first stained for surface markers and next RBC-depleted using IOTest 3 Lysing Solution (Beckman Coulter). Bone marrow, blood and fetal liver cells were stained in PBS+0.5%FCS for 20 min on ice. To identify bone marrow lineage positivity (Lin^+), cells were co-stained with biotin-labelled antibodies against Gr1 (RB6-8C5), Mac1 (M1/70), Ter119 (TER-119), CD3e (145-2C11), CD4 (GK1.5), CD8 (53-6.7) and B220 (RA3-6B2) (all from BD), followed by incubation with Pacific Orange-conjugated streptavidin (Life Technologies). For fetal liver analysis, anti-Mac1 was excluded from the lineage cocktail as this marker is expressed in fetal hematopoietic stem cells.[2] In addition to the lineage cocktail, the following antibodies were used to identify HSPCs: Pacific Blue anti-Sca1 (D7), AF700 or PE anti-CD48 (HM48-1), PE-Cy7 anti-CD150 (TC15-12F12.2), PE anti-CD34 (HM34) (all from Biolegend), APC or PE-CF594 anti-c-Kit (2B8) and APC-Cy7 anti-CD16/32 (2.4G2) (all from BD). To analyze differentiated cells, we used APC anti-Gr1 (RB6-8C5), PE-Cy7 anti-Mac1 (M1/70) (both from Biolegend) and eFluor450 anti-B220 (RA3-6B2, eBioscience). Erythroid subsets were identified by staining with PE anti-CD71 (C2, BD) and Ter119 (TER-119, Biolegend). Dead cells were excluded based on 7-AAD staining (Biolegend). Apoptotic cells were identified with APC annexin V (BD) according to the manufacturer's protocol. For cell cycle and p53 analysis, cells were stained for surface markers, then permeabilized using Cytofix/Cytoperm Fixation/Permeabilization Solution Kit (BD) following the

manufacturer's recommendations and finally stained with PE anti-Ki67 (B56, BD) and 7-AAD (cell cycle analysis) or with AF647 anti-p53 (1C12, Cell Signaling Technology). For all FACS analysis, events were recorded using a BD LSR II Flow Cytometer and analyzed with FlowJo 7.6.5 software (Tree Star). Cells were sorted with a BD FACSAria III.

Bone Marrow Morphology

For morphological studies, cytospin preparations were obtained from $5x10^5$ bone marrow cells per transplanted mouse and stained with May-Grünwald-Giemsa as previously reported.[3]

Quantitative PCR

Cells were sorted in TRIzol Reagent (Life Technologies) and RNA was extracted following the manufacturer's instructions, with addition of 25 µg linear polyacrylamide (Genelute LPA; Sigma Aldrich) as RNA carrier. Genomic DNA was eliminated by treatment with RQ1 RNase-free DNase (Promega). First strand cDNA was synthesized from poly(A)$^+$-selected RNA using SuperScript III First-Strand Synthesis System (Life Technologies). Real-Time PCR reactions were prepared with Fast SYBR Green Master Mix (Life Technologies) using the primers listed in Online Supplementary Table S1 and run on a 7500 Fast Real-Time PCR System (Life Technologies).

Table S1. Oligonucleotide primers used in this study.

Application	Target	Allele	Primer ID	Sequence	Amplicon size, bp
Genotyping	*Sbds*	Wild type	a b	CCAGGGTCACGTTAATACAAACC TGAGTTTCAATCCTCAGCATCC	329
		Floxed	a b	CCAGGGTCACGTTAATACAAACC TGAGTTTCAATCCTCAGCATCC	450
		Recombined	c d	TAAAACAAAGCTGCGGTCAAGA ATCCTCAGCATCCCGAACAA	319
	Cebpa	Wild type	e f	GCTCTAAGACCCAGCAGGC CGGCTCCACCTCGTAGAAGTC	272
		Cre	g h	CGCTAAGGATGACTCTGGT GTCTCAAGGAGAAACCACCAC	487
	Rosa 26	Wild type	i j	ACCTTTCTGGGAGTTCTCTGCTG GGAGCGGGAGAAATGGATATG	488
		EYFP	i k	ACCTTTCTGGGAGTTCTCTGCTG GCGAAGAGTTTGTCCTCAACC	200
		Recombined	i l	ACCTTTCTGGGAGTTCTCTGCTG GCTCCTCGCCCTTGCTCA	400
Quantitative RT-PCR	*Gapdh*		m n	AGGTCGGTGTGAACGGATTTG TGTAGACCATGTAGTTGAGGTCA	123
	Sbds		o p	GCGCTTCGAAATCGCCTG TCTGGTCGTCTGTCCCAAATG	167

Table S2. Complete loss of *Sbds* in *Cebpa*-expressing cells is lethal during mouse development.

Time of DNA isolation	Crossing	Genotype	Expected frequency†	No. pups
P7	**$Sbds^{f/+}$ $Cebpa^{cre/+}$ x $Sbds^{f/+}$ $Cebpa^{cre/+}$**	$Sbds^{+/+}$ $Cebpa^{+/+}$	1/12	7/59
	***P* = 0.0018**	$Sbds^{+/+}$ $Cebpa^{cre/+}$	1/6	18/59
	11 crossings	$Sbds^{f/+}$ $Cebpa^{+/+}$	1/6	8/59
	Average litter size = 5.36	$Sbds^{f/+}$ $Cebpa^{cre/+}$	1/3	23/59
		$Sbds^{f/f}$ $Cebpa^{+/+}$	1/12	3/59
		$Sbds^{f/f}$ $Cebpa^{cre/+}$	1/6	0/59
P7	**$Sbds^{f/f}$ $Cebpa^{+/+}$ x $Sbds^{f/+}$ $Cebpa^{cre/+}$**	$Sbds^{f/+}$ $Cebpa^{+/+}$	1/4	11/33
	***P* = 0.0043**	$Sbds^{f/+}$ $Cebpa^{cre/+}$	1/4	8/33
	5 crossings	$Sbds^{f/f}$ $Cebpa^{+/+}$	1/4	14/33
	Average litter size = 6.25	$Sbds^{f/f}$ $Cebpa^{cre/+}$	1/4	0/33
P7	**$Sbds^{f/+}$ $Cebpa^{cre/+}$ x $Sbds^{f/+}$ $Cebpa^{+/+}$**	$Sbds^{+/+}$ $Cebpa^{+/+}$	1/8	5/36
	***P* = 0.1047**	$Sbds^{+/+}$ $Cebpa^{cre/+}$	1/8	4/36
	5 crossings	$Sbds^{f/+}$ $Cebpa^{+/+}$	1/4	9/36
	Average litter size = 7.20	$Sbds^{f/+}$ $Cebpa^{cre/+}$	1/4	9/36
		$Sbds^{f/f}$ $Cebpa^{+/+}$	1/8	9/36
		$Sbds^{f/f}$ $Cebpa^{cre/+}$	1/8	0/36
E14.5	**$Sbds^{f/f}$ $Cebpa^{+/+}$ x $Sbds^{f/+}$ $Cebpa^{cre/+}$**	$Sbds^{f/+}$ $Cebpa^{+/+}$	1/4	12/49
	***P* = 0.4175**	$Sbds^{f/+}$ $Cebpa^{cre/+}$	1/4	9/49
	5 crossings	$Sbds^{f/f}$ $Cebpa^{+/+}$	1/4	17/49
	Average litter size = 9.80	$Sbds^{f/f}$ $Cebpa^{cre/+}$	1/4	11/49

Cumulative frequencies of litters obtained from intercrossing $Sbds^{f/+}$ $Cebpa^{cre/+}$ $R26^{YFP/+}$mice. The genotype of the parents and the offspring is shown. The R26 genotype is omitted for simplicity. †$Cebpa^{cre/cre}$ mice are not viable due to the complete absence of *Cebpa* coding sequence in the cre allele[4]. *P* values refer to Pearson's chi-squared test.

Table S3. Transcriptional signatures for translation and lineage progression in *Sbds*-deficient MC-MMs.

Cellular process	Data set	Enrichment	Size	ES	NES	NOM p-val	FDR q-val
Translation	BILANGES_RAPAMYCIN_SENSITIVE_VIA_TSC1_AND_TSC2	Mutants	72	0.698	1.611	<0.001	0.2322
	BILANGES_SERUM_RESPONSE_TRANSLATION	Mutants	35	0.701	1.550	0.035	0.1657
	PENG_RAPAMYCIN_RESPONSE_DN	Mutants	243	0.613	1.511	<0.001	0.1753
	REACTOME_TRANSLATION	Mutants	140	0.788	1.477	<0.001	0.1926
	BILANGES_SERUM_AND_RAPAMYCIN_SENSITIVE_GENES	Mutants	64	0.796	1.431	0.021	0.2104
	MENSSEN_MYC_TARGETS	Mutants	52	0.676	1.397	<0.001	0.2450
	REACTOME_SRP_DEPENDENT_COTRANSLATIONAL_PROTEIN_TARGETING_TO_MEMBRANE	Mutants	102	0.826	1.391	0.021	0.2484
	REACTOME_ACTIVATION_OF_THE_MRNA_UPON_BINDING_OF_THE_CAP_BINDING_COMPLEX_AND_EIFS_AND_SUBSEQUENT_BINDING_TO_43S	Mutants	54	0.759	1.390	<0.001	0.2458
Undifferentiated state	BHATTACHARYA_EMBRYONIC_STEM_CELL	Mutants	85	0.575	1.601	<0.001	0.2029
	JUBAN_TARGETS_OF_SPI1_AND_FLI1_DN	Mutants	90	0.582	1.572	<0.001	0.1544
	MUELLER_PLURINET	Mutants	295	0.535	1.539	<0.001	0.1572
	PARK_HSC_AND_MULTIPOTENT_PROGENITORS	Mutants	50	0.504	1.480	0.086	0.1915
	IVANOVA_HEMATOPOIESIS_INTERMEDIATE_PROGENITOR	Mutants	147	0.637	1.469	<0.001	0.1927
	BYSTRYKH_HEMATOPOIESIS_STEM_CELL_AND_BRAIN_QTL_CIS	Mutants	64	0.524	1.403	<0.001	0.2396
	SCHURINGA_STAT5A_TARGETS_DN	Mutants	15	0.478	1.397	0.026	0.2457
	RAMALHO_STEMNESS_UP	Mutants	207	0.531	1.386	<0.001	0.2487
	XU_RESPONSE_TO_TRETINOIN_AND_NSC682994_DN	Mutants	15	0.750	1.383	<0.001	0.2461
Myeloid differentiation	LIAN_NEUTROPHIL_GRANULE_CONSTITUENTS	Controls	24	-0.556	-1.719	<0.001	0.0619
	JAATINEN_HEMATOPOIETIC_STEM_CELL_DN	Controls	214	-0.561	-1.718	<0.001	0.0610
	IVANOVA_HEMATOPOIESIS_MATURE_CELL	Controls	294	-0.582	-1.644	<0.001	0.0820
	PID_AMB2_NEUTROPHILS_PATHWAY	Controls	40	-0.532	-1.612	<0.001	0.1081
	REACTOME_DEGRADATION_OF_THE_EXTRACELLULAR_MATRIX	Controls	27	-0.529	-1.601	<0.001	0.1104
	BROWN_MYELOID_CELL_DEVELOPMENT_UP	Controls	168	-0.665	-1.590	<0.001	0.1221
	TAVOR_CEBPA_TARGETS_UP	Controls	49	-0.503	-1.580	<0.001	0.1229
	PID_INTEGRIN_A9B1_PATHWAY	Controls	25	-0.575	-1.567	<0.001	0.1368
	KEGG_HEMATOPOIETIC_CELL_LINEAGE	Controls	80	-0.460	-1.557	<0.001	0.1438
	SA_MMP_CYTOKINE_CONNECTION	Controls	15	-0.629	-1.542	<0.001	0.1595
	XU_RESPONSE_TO_TRETINOIN_UP	Controls	15	-0.605	-1.478	<0.001	0.1878
	NAKAJIMA_EOSINOPHIL	Controls	27	-0.640	-1.477	0.027	0.1885
	BIOCARTA_CCR3_PATHWAY	Controls	23	-0.670	-1.467	<0.001	0.1930
	ZHOU_INFLAMMATORY_RESPONSE_LPS_UP	Controls	373	-0.380	-1.443	<0.001	0.2240
	KAMIKUBO_MYELOID_CEBPA_NETWORK	Controls	80	-0.457	-1.417	<0.001	0.2492

Curated data sets significantly enriched in *Sbds f/f* (mutants) or +/+ (controls) are shown (FDR<0.25, GSEA comparison to the C2 MSigDB collection). ES: enrichment score. NES: normalized enrichment score. NOM p-val: nominal p-value. FDR q-val: False Discovery Rate q-value.

Table S4. Enrichment of GO-terms for ribosome biogenesis in *Sbds*-deficient MC-MMs.

Data set	Enrichment	Size	ES	NES	NOM p-val	FDR q-val
REGULATION_OF_TRANSLATIONAL_INITIATION	Mutants	28	0.681	1.520	<0.001	0.1831
TRANSCRIPTION_FROM_RNA_POLYMERASE_III_PROMOTER	Mutants	17	0.703	1.523	0.032	0.1869
RIBOSOME_BIOGENESIS_AND_ASSEMBLY	Mutants	17	0.859	1.525	<0.001	0.2012
NUCLEOLUS	Mutants	119	0.700	1.551	<0.001	0.2068
RIBONUCLEOPROTEIN_COMPLEX	Mutants	141	0.672	1.589	<0.001	0.2127
RIBONUCLEOPROTEIN_COMPLEX_BIOGENESIS_AND _ASSEMBLY	Mutants	83	0.664	1.552	<0.001	0.2166
PROTEIN_RNA_COMPLEX_ASSEMBLY	Mutants	64	0.601	1.492	<0.001	0.2168
RRNA_METABOLIC_PROCESS	Mutants	15	0.845	1.589	<0.001	0.2306
TRANSLATIONAL_INITIATION	Mutants	36	0.640	1.455	<0.001	0.2368
NUCLEOLAR_PART	Mutants	17	0.783	1.467	<0.001	0.2414
RIBOSOME	Mutants	38	0.825	1.435	<0.001	0.2420

GO gene sets related to ribosome maturation and translation are significantly enriched in *Sbds f/f* (mutants) (FDR<0.25, GSEA comparison to the C5 MSigDB collection). ES: enrichment score. NES: normalized enrichment score. NOM p-val: nominal p-value. FDR q-val: False Discovery Rate q-value.

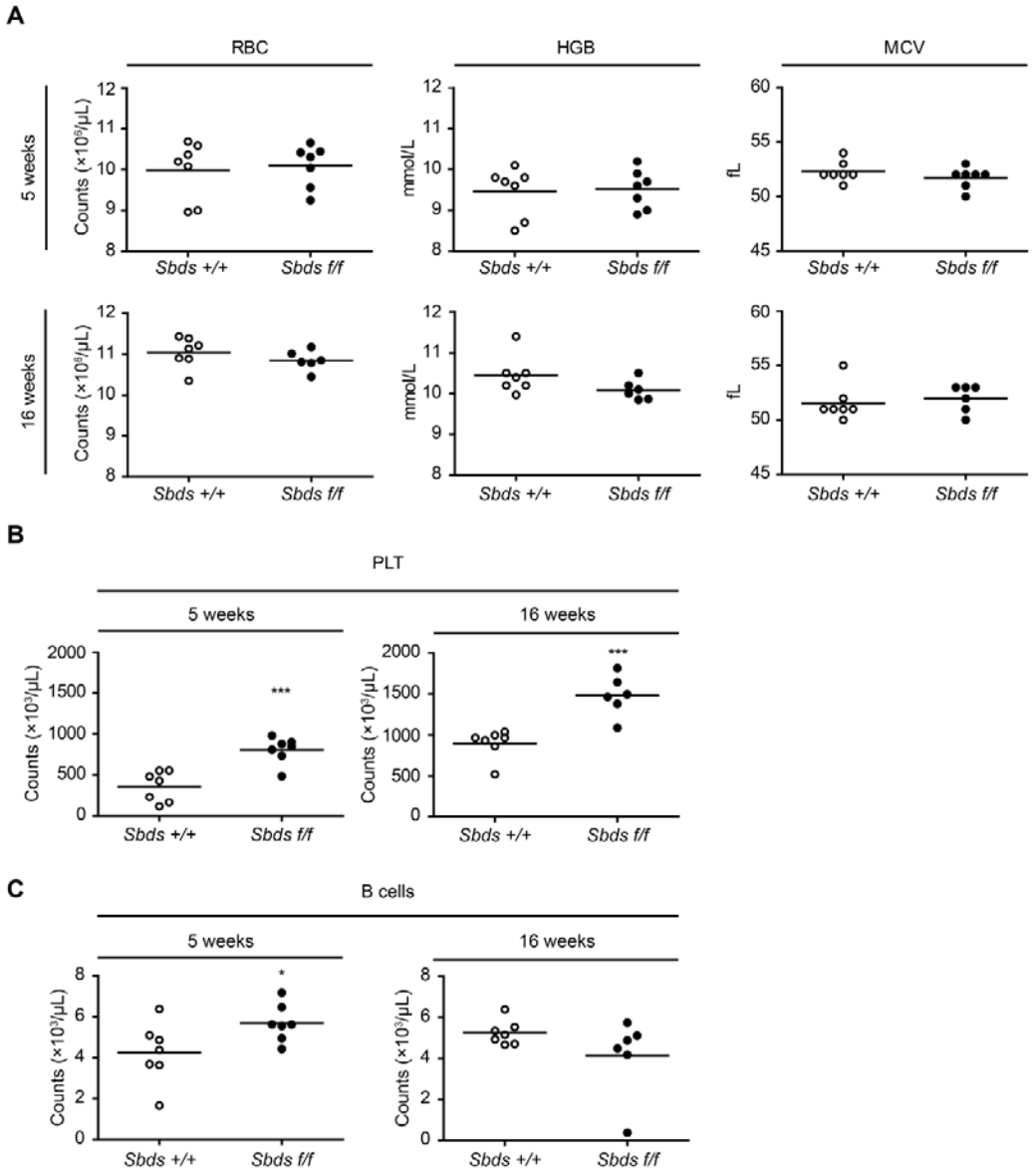

Figure S1. Effects of *Sbds* deletion from *Cebpa*-expressing hematopoietic cells on peripheral blood cell numbers.

(A) Normal levels of red blood cells counts (RBC), hemoglobin (HGB) and mean corpuscular volume (MCV) in mice injected with *Sbds* +/+ or *f/f* cells. (B) Platelet counts (PLT) in the peripheral blood. (C) Numbers of $B220^{+}$ lymphocytes (B cells) in the peripheral blood. Each circle represents one recipient mouse. Data is presented at 5 and 16 weeks after transplantation. * $P < 0.05$. *** $P < 0.001$.

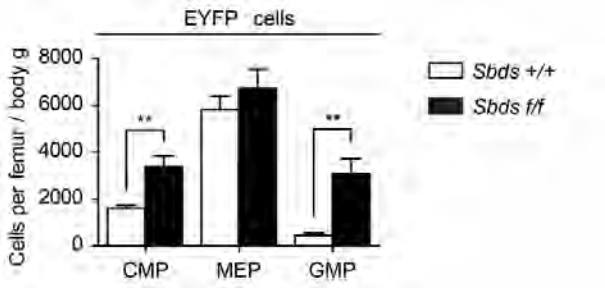

Figure S2. Expansion of EYFP$^-$ progenitors in *Sbds f/f* recipients.

Absolute counts of EYFP$^-$ progenitors in transplanted mice. Data is mean ± s.e.m. ** $P < 0.01$.

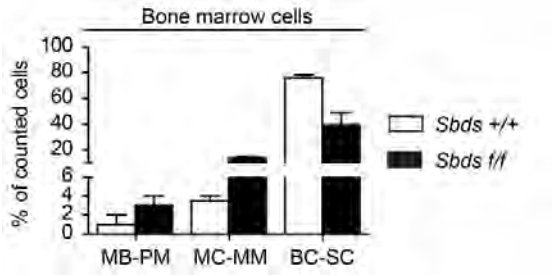

Figure S3. Increased frequency of MC-MMs and loss of mature neutrophils in *Sbds f/f* recipients. Evaluation of myeloid differentiation stages in bone marrow cytospins from *Sbds f/f* and +/+ recipients (*n* = 2). MB-PM: myeloblasts-promyelocytes. MC-MM: myelocytes-metamyelocytes. BC-SC: band cells-segmented cells. Data is mean ± s.e.m.

References

1. Raaijmakers MH, Mukherjee S, Guo S, et al. Bone progenitor dysfunction induces myelodysplasia and secondary leukaemia. *Nature*. 2010;**464**(7290):852-857.

2. Morrison SJ, Hemmati HD, Wandycz AM, Weissman IL. The Purification and Characterization of Fetal Liver Hematopoietic Stem-Cells. *Proc Natl Acad Sci U S A*. 1995;**92**(22):10302-10306.

3. Nishimoto N, Arai S, Ichikawa M, et al. Loss of AML1/Runx1 accelerates the development of MLL-ENL leukemia through down-regulation of p19(ARF). *Blood*. 2011;**118**(9):2541-2550.

4. Wölfler A, Oorschot AADV, Haanstra JR, et al. Lineage-instructive function of C/EBP alpha in multipotent hematopoietic cells and early thymic progenitors. *Blood*. 2010;**116**(20):4116-4125.